Published in final edited form as:
Nature. 2007 August 23; 448(7156): 894–900.

Cortico-striatal synaptic defects and OCD-like behaviors in SAPAP3 mutant mice

Jeffrey M. Welch[1,*], **Jing Lu**[1,2,*], **Ramona M. Rodriguiz**[3], **Nicholas C. Trotta**[1], **Joao Peca**[1,4], **Jin-Dong Ding**[5], **Catia Feliciano**[1,6], **Meng Chen**[7], **J. Paige Adams**[8], **Jianhong Luo**[2], **Serena M. Dudek**[8], **Richard J. Weinberg**[5], **Nicole Calakos**[1,7], **William C. Wetsel**[3], and **Guoping Feng**[1]

1*Department of Neurobiology, Duke University Medical Center, Durham, North Carolina 27710, USA*

2*Department of Neurobiology, Zhejiang University School of Medicine, Hangzhou, Zhejiang 310058, China*

3*Department of Psychiatry and Behavioral Sciences, Cell Biology, Neurobiology, and Mouse Behavioral and Neuroendocrine Analysis Core Facility, Duke University Medical Center, Durham, North Carolina 27710, USA*

4*Center for Neuroscience and Cell Biology, University of Coimbra, Coimbra, Portugal*

5*Department of Cell and Developmental Biology, University of North Carolina, Chapel Hill, North Carolina 27599, USA*

6*Gulbenkian PhD Programme in Biomedicine, Gulbenkian Science Institute, Portugal*

7*Division of Neurology, Center for Translational Neuroscience, Duke University Medical Center, Durham, North Carolina 27710, USA*

8*National Institute of Environmental Health Sciences, National Institutes of Health, Research Triangle Park, North Carolina 27709, USA*

Abstract

Obsessive-compulsive disorder (OCD) is an anxiety-spectrum disorder characterized by persistent intrusive thoughts (obsessions) and repetitive actions (compulsions). Dysfunction of cortico-striato-thalamo-cortical circuitry is implicated in OCD, though the underlying pathogenic mechanisms are unknown. SAP90/PSD95-associated protein 3 (SAPAP3) is a postsynaptic scaffolding protein at excitatory synapses that is highly expressed in the striatum. Here we show that mice with genetic deletion of SAPAP3 exhibit increased anxiety and compulsive grooming behavior leading to facial hair loss and skin lesions; both behaviors are alleviated by a selective serotonin reuptake inhibitor. Electrophysiological, structural, and biochemical studies of SAPAP3 mutant mice reveal defects in cortico-striatal synapses. Furthermore, lentiviral-mediated selective expression of SAPAP3 in the striatum rescues the synaptic and behavioral defects of SAPAP3 mutant mice. These findings demonstrate a critical role for SAPAP3 at cortico-striatal synapses and emphasize the importance of cortico-striatal circuitry in OCD-like behaviors.

Correspondence should be addressed to: Guoping Feng, Ph.D., Department of Neurobiology, Box 3209, Duke University Medical Center, 401F Bryan Research Building, Research Drive, Durham, NC 27710, Tel. 919-668-1657, Fax 919-668-1891, Email: feng@neuro.duke.edu .

*These authors contributed equally to this work.

Author Contributions

J.M.W., J. Lu, R.M.R., N.C.T., J.P., J-D. D., C.F., M.C., and J.P.A. participated in the design, analysis and execution of experiments. G.F., N.C., W.C.W., J.M.W, R.J.W., S.M.D., and J. Luo participated in the design, analysis and interpretation of experiments.

OCD, a common and incapacitating psychiatric disorder, affects ~2 percent of the world population[1,2]. OCD is characterized by persistent intrusive thoughts (obsessions), repetitive actions (compulsions) and excessive anxiety. Clinical expression of OCD is heterogeneous in the types of obsessions and compulsions, heritability, and co-morbid conditions, likely reflecting heterogeneity in the underlying pathology[3]. In addition, there are many disorders that share features with OCD, termed "OC-spectrum disorders" that include Tourette's syndrome, trichotillomania, and body dysmorphic disorder.

The neurobiological basis of OCD is unclear. However, lesions, functional neuro-imaging, and neuropsychological studies have indicated that the cortico-striato-thalamo-cortical (CSTC) circuitry may play a key role in the pathogenesis of OCD[3-5]. Familial studies of OCD indicate that the risk to first degree relatives is 3-12 times greater than the general population, similar to familial risk rates observed for bipolar disorder and schizophrenia[6-8]. In addition, concordance for OCD is greater among pairs of monozygotic (80-87%) than dizygotic twins (47-50%)[9,10]. However, no genetic factors have yet been identified as a cause of OCD, presumably reflecting etiological heterogeneity within the disorder. While many of the symptoms of OCD can be ameliorated by enhancing serotonin neurotransmission, it is not clear at the cellular level whether defects in the serotonergic system are the primary cause[3-5]. Indeed, dopaminergic and glutamatergic neurotransmitter systems have also been implicated[5,11]. Here we show that targeted deletion of SAPAP3 in mice leads to a behavioral phenotype similar to OCD: compulsive over-grooming behavior, increased anxiety, and response to selective serotonin reuptake inhibitors (SSRIs). In these mutant mice, we have identified defects at cortico-striatal synapses, part of the circuitry implicated in OCD, and we show that selective expression of SAPAP3 in the striatum rescues the synaptic and behavioral defects. These findings suggest that defects in excitatory transmission at cortico-striatal synapses may underlie some aspects of OCD.

SAPAP3 mutant mice exhibit self-inflicted facial lesions

SAPAP family proteins were originally identified as postsynaptic density (PSD) components that interact with the PSD95 and Shank families of proteins[12-13], two other multi-domain postsynaptic scaffolding proteins at excitatory synapses. Together, these three groups of proteins are thought to form a key scaffolding complex that regulates the trafficking and targeting of neurotransmitter receptors and signaling molecules to the postsynaptic membrane of excitatory synapses[14-16]. There are four highly homologous genes in the SAPAP family[13]. Of these, SAPAP1, 3, and 4 are highly, but differentially, expressed in several regions of the brain[17,18]. Notably, SAPAP3 is the only member highly expressed in the striatum. To facilitate study of the *in vivo* function of SAPAP proteins at synapses, we generated knockout mice for the SAPAP3 gene using homologous recombination in mouse ES cells (Supplementary Fig. S1a-d). Mice homozygous for SAPAP3 deletion ($SAPAP3^{-/-}$) were born at the expected Mendelian rate, grew to adulthood with body weights similar to wildtype mice, and were fertile. Anatomical and histological analyses of brain showed that $SAPAP3^{-/-}$ mice were grossly normal (data not shown).

By the age of 4-6 months, however, $SAPAP3^{-/-}$ mice developed lesions on their head, neck, and snout regions (Fig. 1a). This phenotype was 100% penetrant. Lesions were usually first noticed as a patch of hairless skin under the eyes or swelling of the snout, progressing to relatively symmetric bilateral lesions encompassing large parts of the neck and head. $SAPAP3^{-/-}$ mice developed lesions regardless of whether they were housed alone or with cagemates. Lesions were not observed on wildtype or heterozygous mice even when housed in the same cage with $SAPAP3^{-/-}$ mice from birth, thereby excluding the possibility that lesions were caused by allogrooming or were the result of aggressive encounters with other

SAPAP3$^{-/-}$ mice. In fact, SAPAP3$^{-/-}$ mice were not observed to behave aggressively, but were often seen engaged in self-grooming whether they were housed alone or in groups.

Given the obvious lesions on the SAPAP3$^{-/-}$ mice, we tested the possibility that their lesions might be caused by peripheral cutaneous defects, such as inflammation or abnormal afferent sensation. We examined facial skin from pre-lesion SAPAP3$^{-/-}$ mice that exhibited increased grooming. Histological analysis of skin did not reveal any anatomical differences among wildtype, SAPAP3$^{+/-}$ and SAPAP3$^{-/-}$ mice, and no lymphocytic or granulocytic infiltration was observed (Supplementary Fig. S1e, f). We did, however, find lymphocytic/granulocytic infiltration in skin with lesions, likely due to injury and infection (Supplementary Fig. S1g). No differences were detected in sensory innervation among wildtype, SAPAP3$^{+/-}$ and SAPAP3$^{-/-}$ mice; hair-nerve end organs, lobular corpuscle-like nerve endings, and free epidermal nerve endings were present and not different between SAPAP3$^{-/-}$ and control mice (Supplementary Fig. S1h, i). Thus, our examination revealed no obvious peripheral defects that would suggest a cause for the lesions. Together, these findings raised the possibility that SAPAP3$^{-/-}$ mice have excessive and injurious self-grooming behavior.

OCD-like behaviors of SAPAP3 mutant mice

To determine whether SAPAP3$^{-/-}$ mice groom excessively, we continuously videotaped habituated, individually-housed mice for 24 hours. Isolated SAPAP3$^{-/-}$ mice showed dramatically increased grooming bouts and spent significantly more time self-grooming than wildtype littermates (Fig. 1b, c). The increased grooming was present throughout the day, including the period when mice usually sleep (1000 - 1400h). Both mutant mice with facial lesions and mice yet to develop lesions showed similar degrees of increased grooming (Fig. 1d), indicating that the lesion itself was not the cause of increased grooming. We thus conclude that SAPAP3$^{-/-}$ mice have excessive and injurious levels of self-grooming, a phenotype reminiscent of compulsive behaviors.

Because the SAPAP3$^{-/-}$ mice exhibited a compulsive-like behavior, we considered whether their phenotypes further resemble OC-spectrum disorders. We therefore examined other OCD-like behaviors that are measurable in mice: increased anxiety and response to typical pharmacological agents. To test whether SAPAP3$^{-/-}$ mice exhibit increased anxiety, we conducted open field, dark-light emergence, and elevated zero maze tests. In the open field, mice with anxiety-like phenotypes tend to stay along the walls, avoiding the center zone. SAPAP3$^{-/-}$ mice spent much less time exploring the center area than wildtype littermates (Fig. 1e). However, activities along the walls and corners, areas believed to be less stressful, were not different between wildtype and SAPAP3$^{-/-}$ mice (Fig. 1f). In the dark-light emergence test, the latency to cross from a dark into a brightly lit chamber (a stressful environment), and the time spent in the brightly lit chamber were examined. SAPAP3$^{-/-}$ mice took longer to cross from the dark to the lit chamber and spent less time in the lit chamber than wildtype controls (Fig. 1g, h), though total activity in the chambers was similar between wildtype and SAPAP3$^{-/-}$ mice (Fig. 1i). Finally, in the elevated zero maze test, we found that SAPAP3$^{-/-}$ mice took longer to cross into the open areas (riskier environment) and spent significantly less time exploring the open areas compared to wildtype controls (Fig. 1j, k), whereas total activity was not different between the two genotypes (Fig. 1l). Together, these results indicate that SAPAP3$^{-/-}$ mice have an anxiety-like phenotype.

We next evaluated whether drugs used to treat OCD would be effective in reducing the abnormal behavior in SAPAP3$^{-/-}$ mice. SSRIs are a first-line treatment for OCD; although their mechanism of action is not well understood, these drugs alleviate symptoms in approximately 50% of OCD patients[3]. Fluoxetine treatment for 6 days (once per day at 5mg/kg, i.p.) did not affect grooming behavior of wildtype mice. However, this treatment significantly reduced the

excessive grooming in SAPAP3$^{-/-}$ mice (Fig. 2a). Furthermore, fluoxetine dramatically reduced anxiety-like behaviors in SAPAP3$^{-/-}$ mice in the dark-light emergence test without affecting their total activity (Fig. 2b, c). In contrast, a single injection of fluoxetine (5mg/kg, i.p.) had no effects on their excessive grooming behavior (Fig. 2d). Thus, SAPAP3$^{-/-}$ mice exhibit compulsive-like grooming and increased anxiety, both of which are alleviated by 6 days of fluoxetine treatment.

Altered cortico-striatal synaptic transmission in SAPAP3$^{-/-}$ mice

The observations that SAPAP3 is the only member of the SAPAP family highly expressed in the striatum (Fig. 3a) and that SAPAP3$^{-/-}$ mice show OCD-like behaviors suggest that there may be defects in striatal neurotransmission in SAPAP3$^{-/-}$ mice. Since SAPAPs are postsynaptic proteins of excitatory synapses[12,17] that directly bind PSD95 family proteins, which are known to regulate the trafficking of both AMPA- and NMDA-type glutamate receptors (AMPAR and NMDAR, respectively)[19-21], we focused on cortico-striatal synapses, which constitute the large majority of glutamatergic synapses in the striatum. We performed extracellular recordings from acute striatal brain slices. A field recording electrode was placed in the dorso-lateral striatum and a stimulating electrode was placed nearby in the corpus callosum. Recordings were obtained in the presence of picrotoxin, a $GABA_A$ receptor antagonist, to block contaminating responses from intra-striatal GABAergic circuitry. We found that field excitatory postsynaptic potentials (fEPSP) were significantly reduced in SAPAP3$^{-/-}$ mice compared to wildtype littermates (Fig. 3b). Axonal excitability and presynaptic function were not different from wildtype, as indicated by the slope of the input-output curves normalized to the peak response, the relationship of stimulation intensity to the amplitude of the action potential component (NP1; Supplementary Fig. S2a, b), and paired-pulse ratios (Fig. 3c), suggesting that the reduction in total field responses was likely due to a postsynaptic impairment in synaptic transmission.

We next evaluated NMDAR-mediated responses by recording in the presence of an AMPAR antagonist (NBQX) and the NMDAR co-factor glycine, in the absence of magnesium. Surprisingly, in contrast to the reduction we observed in the total fEPSP amplitude, which is dominated by AMPAR transmission under these conditions, the NMDAR-dependent fEPSPs were elevated in SAPAP3$^{-/-}$ mice (Fig. 3d, e). These findings indicate a differential effect of SAPAP3 deletion on extracellular field potentials dependent upon AMPAR and NMDAR activity. We further tested whether the synaptic defects are unique to the striatum, by examining synaptic transmission in the hippocampus, in which SAPAP1, 3 and 4 are highly expresed[17,18]. We found no defects in CA3-CA1 hippocampal basal synaptic transmission in SAPAP3$^{-/-}$ mice (Supplementary Fig. S2c, d), likely reflecting functional redundancy or compensation by other members of the SAPAP family. Together these findings identify an important role for SAPAP3 in postsynaptic glutamatergic synaptic function at cortico-striatal synapses.

Altered NMDAR composition of the PSD in striatum

To investigate the potential role of SAPAP3 in postsynaptic assembly, we examined the levels of a select group of PSD proteins that directly or indirectly interact with SAPAPs using biochemically-purified PSD fractions from the striatum of wildtype and SAPAP3$^{-/-}$ mice. We found no significant differences in the levels of PSD95, PSD93, or Shank proteins in the striatal PSD between the genotypes (Fig. 4a, b). However, the level of NR1, the obligatory subunit of the NMDAR, was significantly increased (Fig. 4a, b). This result is consistent with our data from extracellular recordings in the striatum, which showed increased NMDAR field potential responses. While we cannot exclude the possibility that the larger NMDAR-dependent fEPSPs include a contribution from activated conductances other than NMDARs (a limitation of

extracellular recordings), our electrophysiological data in combination with these biochemical findings suggest that an increase in NMDARs in the PSD may result in increased synaptic NMDAR activity in SAPAP3$^{-/-}$ mice. Interestingly, we also found that the level of NR2B, the "juvenile" subunit of the NMDAR, was significantly increased in the PSD of SAPAP3$^{-/-}$ mice, whereas NR2A, the "adult" subunit, was significantly reduced (Fig. 4a, b). In contrast, we found no significant changes in the overall levels of NR1, NR2A and NR2B subunits in the total striatal lysate (Supplementary Fig. S3a, b), suggesting that the changes in these subunits occur exclusively at the PSD. Synaptic NMDARs are known to undergo a developmental switch from predominantly NR1/NR2B to NR1/NR2A or NR1/NR2A/NR2B during the first two postnatal weeks of life[22-27]. Although the underlying molecular mechanisms of this developmental switch are not well understood, postsynaptic scaffolding proteins, including the PSD95 and SAPAP family of proteins, have been implicated in this process[28-31]. Our data indicate that the NMDAR subunit composition at cortico-striatal synapses of adult SAPAP3$^{-/-}$ mice is similar to that of wildtype juvenile mice[27,28], suggesting that SAPAP3 may play an important role in synaptic NMDAR subunit switching and maturation at cortico-striatal synapses.

Structure of cortico-striatal synapses in SAPAP3 mutant mice

To determine whether these electrophysiological and biochemical defects are accompanied by morphological changes, we examined the spine density of medium spiny neurons (MSNs) in the striatum using both Golgi staining and DiI filling by Diolistics. We found similar spine densities on MSNs in SAPAP3$^{-/-}$ and wildtype mice at P21 (Supplementary Fig. S3c-e) and in adults (data not shown), indicating that spine formation and maintenance were not affected by the lack of SAPAP3 proteins.

We next examined whether deletion of SAPAP3 affects PSD ultrastructure at cortico-striatal synapses using electron microscopic (EM) analysis to measure the length and thickness of the PSD in the striatum (Fig. 4c, d). We found no significant difference in length of the PSD between SAPAP3$^{-/-}$ and wildtype mice (Fig. 4e). The PSD is reported to exhibit a laminar organization: NMDARs, scaffolding proteins, and signaling proteins reside in the electron-dense layer near the synaptic membrane, while proteins linked to trafficking and the actin cytoskeleton reside in the filamentous fringe towards the cytoplasm[32]. Accordingly, we independently measured the thickness of the "dense layer" and the fringe "light layer". We found a small but significant reduction in thickness of the dense layer but not the light layer (Fig. 4f, g) of the PSD in striatal synapses in SAPAP3$^{-/-}$ mice, suggesting a subtle defect in the structure of the postsynaptic complex. This finding is consistent with the proposed role of SAPAP3 as a postsynaptic scaffolding protein at excitatory synapses[12,17].

Lentiviral-mediated expression of SAPAP3 in the striatum rescues behavioral and synaptic defects of mutant mice

Our findings of altered cortico-striatal synaptic function and structure in SAPAP3 mutant mice, along with pre-existing evidence for the role of striatal circuitry in the pathogenesis of OC-spectrum disorders led us to ask whether loss of SAPAP3 in the striatum was critical for the phenotypes of SAPAP3$^{-/-}$ mice. We therefore investigated whether selective expression of SAPAP3 in the striatum was sufficient to rescue the phenotypes of SAPAP3$^{-/-}$ mice. We generated lentiviral vectors that express either green fluorescent protein (GFP) alone or a GFP-SAPAP3 fusion protein. GFP was fused to SAPAP3 at the amino-terminus, a region with no known protein-protein interaction sites or motifs. As expected, GFP-SAPAP3 fusion proteins properly localized to synapses when transfected into cultured neurons (Supplementary Fig. S4a).

Lentiviruses expressing either GFP or GFP-SAPAP3 were delivered to the striatum of SAPAP3$^{-/-}$ mice by bilateral microinjections at postnatal day 7. To minimize injury and maximize lentiviral infection, we gave injections at one anterior and one posterior site per hemisphere and delivered lentivirus to 8 locations per hemisphere by injection of lentivirus along the needle path (Fig. 5a; see Methods). Sustained expression of GFP and GFP-SAPAP3 was observed in both dorsal and ventral striatum in post-mortem examination of brains at the end of the study (Fig. 5b-e'; Supplementary Fig. S4b, c).

At 4-6 months after injection, behavioral analyses were conducted to assess grooming, facial lesions, and anxiety-like behaviors. When examined by continuous videotaping, excessive grooming was markedly reduced in SAPAP3$^{-/-}$ mice injected with GFP-SAPAP3 lentivirus in comparison to SAPAP3$^{-/-}$ mice injected with the control GFP lentivirus (Fig. 5f). Moreover, facial lesion severity was also significantly reduced in SAPAP3$^{-/-}$ mice injected with GFP-SAPAP3 lentivirus (Fig. 5g, h). All 8 SAPAP3$^{-/-}$ mice injected with the control GFP lentivirus developed open skin lesions (6 with large, 1 with medium, and 1 with small open wounds). In contrast, only 3 of the 8 SAPAP3$^{-/-}$ mice injected with GFP-SAPAP3 lentivirus developed open skin lesions (1 with large, 1 with medium, and 1 with small open wounds), while 2 had small hairless patches and 3 had normal skin conditions (Fig. 5i). Furthermore, SAPAP3$^{-/-}$ mice injected with GFP-SAPAP3 lentivirus also showed reduced anxiety-like behavior in the dark-light emergence test (Fig. 5j, k) with no change in total activity (data not shown). Finally, lentiviral-mediated expression of GFP-SAPAP3 in the striatum also rescued defects in cortico-striatal synaptic transmission in SAPAP3$^{-/-}$ mice (Fig. 5l, m). Together, these data show that early postnatal expression of GFP-SAPAP3 selectively in the striatum is sufficient to alleviate the major manifestations of the OCD-like phenotype in SAPAP3$^{-/-}$ mice.

Discussion

Although dysfunction of cortico-striato-thalamo-cortical circuitry has been widely implicated in OC-spectrum disorders, the nature of this dysfunction remains unclear. Our study of SAPAP3 mutant mice has identified an important role for SAPAP3 at cortico-striatal synapses and, although there are inherent limitations of evaluating thought content in mice, our study further suggests that cortico-striatal synaptic defects may be central to the genesis of OCD-like behaviors. These conclusions are supported by several lines of evidence. First, SAPAP3$^{-/-}$ mice exhibit OCD-like behaviors: excessive time spent on performing a ritualistic action to the point of being self-injurious, increased anxiety-like behaviors, and response of these manifestations to SSRIs. Second, SAPAP3 is expressed at excitatory, but not inhibitory, synapses[15]. Third, SAPAP3 is the only member of the SAPAP3 family that is highly expressed in the striatum. Fourth, SAPAP3 mutant mice have reduced cortico-striatal synaptic transmission and an NMDAR subunit composition suggestive of immature cortico-striatal synapses. Finally, selective expression of SAPAP3 in the striatum of SAPAP3$^{-/-}$ mice rescues the synaptic defects and OCD-like behaviors.

Anxiety is attributed primarily to dysfunction of the amygdala and ventral hippocampus. Interestingly, SAPAP3, unlike SAPAP1 and SAPAP4, is not highly expressed in the amygdala (Supplementary Fig. S5a-d), while all 4 members of the SAPAP family are expressed in the ventral hippocampus (Supplementary Fig. S5e-h), suggesting that anxiety-like behavior in SAPAP3$^{-/-}$ mice is unlikely to be due to the lack of SAPAP3 in amygdala or ventral hippocampus. The unique expression of SAPAP3 in the striatum and the alleviation of the anxiety-like behavior by lentiviral-mediated expression of GFP-SAPAP3 in the striatum suggest that the anxiety-like behavior in SAPAP3$^{-/-}$ mice originate from striatal defects. Because the amygdala projects to the striatum, it is also possible that some functions of amygdalar-striatal projections are impaired in SAPAP3$^{-/-}$ mice. Additionally, our video surveillance data indicate that SAPAP3 mutant mice have disrupted sleep pattern

(Supplementary Fig. S6), which is alleviated by fluoxetine treatment (Supplementary Fig. S7). This sleep disturbance may also contribute to the anxiety-like behavior in SAPAP3$^{-/-}$ mice.

A principal role of the striatum is to integrate the various inputs arriving from the cortex and use this information to select certain motor and/or cognitive programs (decision making), which are subsequently carried out through the direct and indirect pathways of the basal ganglia[4]. A prominent model for OCD is that an activity imbalance between the direct and indirect pathways leads to behavioral abnormalities of OCD[3], and recent studies have shown that the two pathways are differentially regulated at cortico-striatal synapses[33-35]. We have identified defects in both AMPAR- and NMDAR-dependent synaptic transmission at cortico-striatal synapses. These data are from extracellular field recordings, representing a population average of the effects on individual neurons. If the observed effects are differentially manifested by MSNs in the direct or indirect pathway, an imbalance in activity could be readily envisioned.

Studies of the mechanisms of OC-spectrum disorders have mostly focused on the serotonergic and dopaminergic systems. However, recent genetic association studies of OCD in humans have implicated genes important for glutamatergic neurotransmission[36-38]. Together with our study of SAPAP3 in mice, these observations raise the possibility that defects in excitatory synaptic transmission in the cortico-striatal circuit may contribute to the pathogenesis of OC-spectrum disorders in humans.

METHODS SUMMARY

Behavioral analysis

SAPAP3 knockout mice were generated by homologous recombination in R1 embryonic stem cells using standard procedures[39]. Adult mice age 4-8 months were used for behavioral analyses. For analyses of grooming behaviors[40], habituated, individually housed animals were video-taped for 24 hours under 700 lux (day) and ~2 lux (red light at night) illumination. Tests for anxiety-like behaviors were performed as described[41, 42]. All experiments were done blind to genotypes. Because of the presence of obvious facial lesions in SAPAP3 mutant mice, it is impossible to perform video decoding in a blind manner. To avoid bias, trained individuals unfamiliar with the project (listed in the Acknowledgements) were recruited to decode the videos.

Cortico-striatal electrophysiology

300 μm acute sagittal brain slices from P17-P25 mice were used for all experiments. The field recording electrode was placed in the dorso-lateral striatum and a monopolar stimulation electrode was placed in the corpus callosum. All recordings were performed at 30-32°C and in the presence of picrotoxin and all data were collected and analyzed prior to unblinding of genotypes.

Stereotaxic injection

One week old SAPAP3$^{-/-}$ mice were anesthetized and placed in a mouse head holder. GFP lentivirus or GFP-SAPAP3 lentivirus was bilaterally injected into the striatum through 2 sites at 8 locations per hemisphere. Behavioral analyses were performed 4-6 months after injection.

METHODS

Mice

SAPAP3 knockout mice were generated by homologous recombination in R1 embryonic stem cells using standard procedures. A targeting vector was designed to replace exon 3 (containing

the translation initiation codon) of the SAPAP3 gene with a NEO cassette. Genotypes were determined by PCR of mouse tail DNA, using primer F1 (ATTGGTAGGCAATACCAACAGG) and R1 (GCAAAGGCTCTTCATATTGTTGG) for the wildtype allele (147 base pairs), and F1 and R2 (CTTTGTGGTTCTAAGTACTGTGG; in neo cassette) for the mutant allele (222 base pairs). Primer locations are indicated in Fig. S1.

Grooming behavior[40]

Adult mice age 4-8 months were used. Habituated, individually housed animals were video-taped for 24 hours under 700 lux (day) and ~2 lux (red light at night) illumination. As behaviors were most representative at 0200-0600, 1000-1400, and 1800-2200 hr, these segments were selected for analyses using Noldus Observer software (Leesburg, VA). The total amount of time in each 4-hour segment spent grooming, eating, sleeping, rearing, digging or pushing bedding (shifting) was determined, along with general states of activity. Grooming included all sequences of face-wiping, scratching/rubbing of head and ears, and full-body grooming. Bouts of behavior lasted at least 3 seconds; pauses longer than 3 seconds constituted a new bout. Observer reliability was determined with Cohen's kappa[43].

Anxiety-like behaviors[41, 42]

Zero maze—An elevated zero maze[41] was indirectly illuminated at 60 lux. Testing commenced with an animal being introduced into a closed area of the maze. Behavior was video-taped for 5 min and subsequently scored by trained observers using the Noldus Observer (Nodus Information Technology). Anxiety-like behavior was deduced based upon the percent time spent in the open areas and the latency to enter the open areas. Total activity time in the maze was an indicator of motor activity. Observer reliability was determined with Cohen's Kappa.

Open field—Spontaneous locomotor activity was evaluated over 30 min in an automated Omnitech Digiscan apparatus (AccuScan Instruments, Columbus, OH) as described[44]. Locomotor activity was assessed as total distance traveled (cm). Anxiety-like behavior was defined by the percent time spent in the center as contrasted to percent time spent in the perimeter (thigmotaxis) of the open field.

Dark-Light Emergence Test[45]—Mice were adapted in an adjacent room to low light conditions (~40 lux) and the test room was initially under similar illumination. Testing was conducted in a two-chambered test apparatus (Med-Associates, St. Albans, VT), with one side draped in black cloth (e.g., dark-chamber) and the other illuminated at ~1400 lux (e.g., light-chamber) with a 170 mA high intensity house light and overhead fluorescent lamps. Immediately upon placing the mice into the darkened chamber, the lighted chamber was illuminated and the door between the two chambers was opened. The mice were allowed to freely explore the apparatus for 5 min. The latency to emerge from the darkened into the lighted chamber and the percent time spent in the illuminated chamber were used as indices of anxiety-like behaviors. Total motor activity in the two chambers was measured by infrared beam-breaks.

Fluoxetine treatment

Adult mice 4-6 months of age were injected with fluoxetine (5 mg/kg, i.p.) once a day for one or six days and behaviors were tested 24 hours after the final injection. Grooming and anxiety-like behaviors were tested as described above.

Skin analyses

Hematoxylin and eosin staining was performed on facial skin below the eyes following a standard protocol. For visualization of sensory nerves in skin, SAPAP3 mutant mice were crossed with Thy1GFP-J mice[46]. Mice were perfused transcardially with saline and 4% paraformaldehyde and skin from just below the eyes was dissected and post-fixed for 24 hours. Confocal images were taken from 50 μm cryosections. Skin lesions were scored as follows: 0=normal skin; 1=hairless patches; 2=small open-wound lesions, length < 2mm; 3=moderate open-wound lesions, length 2-4mm; 4=large open-wound lesions, length >4mm.

Cortico-striatal electrophysiology

300 μm acute sagittal brain slices from P17-P25 mice were used for all experiments. Recording perfusion solution contained (in mM): 119 NaCl, 2.5 KCl, 1.2 NaH_2PO_4, 26 $NaHCO_3$, 1 $MgCl_2$, 2 $CaCl_2$, and 0.1 picrotoxin ($GABA_A$ receptor antagonist). Slicing and recovery solutions were identical to perfusion solution except for containing 0.5 $CaCl_2$ and no picrotoxin. APV (50 μM) and NBQX (50 μM) were obtained from Tocris (Ellisville, MO). Solutions were continuously equilibrated with 95% O_2 and 5% CO_2 (pH 7.4) and perfusion flow rate was 2 ml/min. Slices were allowed to recover for a minimum of 1 hr at 30-32°C following slicing. All recordings were performed at 30-32°C.

The field recording electrode was placed in the dorso-lateral striatum and a monopolar stimulation electrode was placed in the corpus callosum. Current was delivered to the stimulating electrode using an A.M.P.I. Stimulus Isolator (A.M.P.I., Israel) for 150 μsec. Three distinct components were resolved in the majority of recordings: stimulation artifact, negative peak 1 (NP1, action potential-derived based on latency, resistance to NBQX and picrotoxin, and sensitivity to tetrodotoxin) and negative peak 2 (NP2, fEPSP based on latency and sensitivity to NBQX; in addition, sensitivity to tetrodotoxin indicates response not due to direct activation by stimulating electrode current). The callosal stimulation site was chosen over an intra-striatal site to minimize activation of non-cortical axons. Data were acquired at 20 kHz and filtered at 2 kHz using MultiClamp 700B amplifier and pClamp 10.0 software (Axon Instruments, Sunnyvale, CA). Data were analyzed offline using Clampfit 10.0 (Axon Instruments). Five consecutive responses were averaged prior to measuring amplitude, slope or area in the respective assays. When amplitudes are reported, similar conclusions were obtained by slope analysis. Paired-pulse responses were evoked using a stimulation intensity that yielded the maximal fEPSP response. Slope values used for paired-pulse ratios refer to slope during the period from 20-80% of the peak response. NMDAR fEPSPs were evoked using the same stimulation intensity that yielded the maximal fEPSP response under the basal recording conditions used to generate the input-output curves. The area of NMDAR field potential responses was measured during a standard 20 millisecond time window beginning approximately 8 milliseconds after stimulation. All data were collected and analyzed prior to unblinding of genotypes. In addition, NMDAR field potential recordings and correlative PSD biochemical studies were performed in two different labs and were unblinded at the same time.

For *in vivo* viral expression rescue experiments, the same slicing, recording, and analysis methods were used as described above except that the stimulating and recording electrodes were placed within the fluorescent green tissue. Only slices where green cells were visible in the dorsolateral recording region were used. Viral rescue experiments were performed and analyzed blinded to the viral identity.

Diolistics

"Bullets" were prepared by coating tungsten particles (Bio-rad) with DiI (Molecular Probes-Invitrogen) dissolved in methylene chloride as described[47]. Mice were perfused transcardially, first with normal saline, and then with buffered 4% paraformaldehyde. Fixed mice were

decapitated and the head was allowed to post-fix for 24-48 hours in buffered 4% paraformaldehyde at 4°C. Brains were dissected and 250 μm coronal slices were cut on a vibratome.

Diolistic filling of individual cells was performed using a standard Bio-Rad biolistic system. Slices were placed into the interior chamber of a Falcon organ tissue culture dish (catalog number 3037) and excess buffer was removed. A Millipore 3.0 μm Isopore filter (catalog number TSTP04704) was placed to rest on top of the tissue culture dish and a Kimwipe was placed on top of the Millipore filter. Bullets were shot through the Kimwipe and filter barrier using a helium charge of 80psi. Individual labeling of 3-15 striatal medium spiny neurons was successful in approximately 50% of slices. Following the diolistic procedure, slices were allowed to incubate in buffer at 4°C for 1-2 hours. Following incubation, slices were immediately mounted and imaged on a confocal microscope.

Lentivirus production and stereotaxic injection

Lentivirus vector was based on FUGW[48] and modified by replacing the ubiquitin promoter with a CMV promoter to improve neuronal expression. GFP was fused to the amino-terminus of SAPAP3 to generate the GFP-SAPAP3 construct. The cDNA clone encoding GFP or GFP-SAPAP3 was placed downstream of the CMV promoter between BamHI and EcoRI sites[48]. Viral particles were produced by transient transfection of 293T cells with the GFP or GFP-SAPAP3 lentiviral vector along with the envelope (VSVg) and packaging (Δ8.9) vectors. High titer viral suspensions were obtained by ultra-centrifugation at 77,000 X g for 90 min.

One week old SAPAP3$^{-/-}$ mice were anesthetized with a mixture of ketamine and xylazine (i.p), and placed in a mouse head holder (David Kopf Instruments, Tujunga, CA). GFP lentivirus or GFP-SAPAP3 lentivirus was bilaterally injected into the striatum through 2 sites at 8 locations per hemisphere. At each of the injection sites, the microinjection needle was advanced to the deepest (ventral) position for the first injection; additional injections were made every 0.3 mm while withdrawing the injection needle. The coordinates from Bregma were: injection site 1, location 1-3: anterior 0.5 mm, mediolateral 1.4 mm, dorsoventral 2.8, 2.5, 2.2 mm; injection site 2, location 4-8: anterior 0.2 mm, mediolateral 1.7 mm, dorsoventral 3.3, 3.0, 2.7, 2.4, 2.1 mm. For each injection location, 90 nl of virus was injected using Nanoject II (Drummond Scientific, Broomall, CA), and the needle was left in place for 3 min after each injection.

EM analysis

Striatal tissues for EM analysis were processed and quantitatively analyzed according to protocols previously described[32]. Synapses with clear membranes (likely to be cut orthogonal to the plane of the synaptic membrane) were photographed at 15,000X magnification. Data collection and analysis were performed by observers blinded to genotypes. For every clearly-defined synapse, data for PSD length and PSD thickness were collected.

PSD preparation and Western blot

PSD fractions of the striatum were prepared as described[17,49], separated on SDS-PAGE and probed with specific antibodies. The relative amount of β-tubulin and β-actin were used as loading controls for quantification. Antibodies for SAPAP3, PSD95, PSD93, Shank and NR2B have been described previously[17,49,50]. Antibodies for NR1 (mouse monoclonal) and NR2A (rabbit polyclonal) were from BD Biosciences (San Jose, CA) and Upstate (Charlottesville, VA), respectively.

Supplementary Material

Refer to Web version on PubMed Central for supplementary material.

Acknowledgements

We thank Jimmy Gross, Kristen Phend and Li Qiu for excellent technical assistance, and Lindsey Phillips, Lien Nguyen, Stacy Greeter, John Wilkins, and Masato Fukui for assistance in behavioral testing and decoding of video tapes. We thank Michael Ehlers for the anti-NR2B antibody and Eunjoon Kim for the anti-Shank antibody. We also thank Marc Caron, Michael Ehlers, Zhigang He, Joshua Sanes, Fan Wang, Anne West and members of the Feng lab for critical reading of the manuscript. This work was supported by grants from NINDS and NIMH to G.F, R.J.W. and N.C.; by unrestricted funds to W.C.W., and by the Intramural Research Program of NIEHS to S.M.D. J.M.W. was supported by an NSF pre-doctoral fellowship and an NIH National Research Service Award. N.C. is a recipient of a Klingenstein Fellowship in the Neurosciences and a NARSAD Young Investigator Award. G.F. is a recipient of a Sloan Fellowship, a Klingenstein Fellowship in the Neurosciences, an EJLB Foundation Scholar Research Program Award, a McKnight Neuroscience of Brain Disorders Award, and a Hartwell Foundation Individual Biomedical Research Award.

References

1. Karno M, Golding JM, Sorenson SB, Burnam MA. The epidemiology of obsessive-compulsive disorder in five US communities. Arch. Gen. Psychiatry 1988;45:1094–1099. [PubMed: 3264144]
2. Torres AR, et al. Obsessive-compulsive disorder: prevalence, comorbidity, impact, and help-seeking in the British national psychiatric morbidity survey of 2000. Am J Psychiatry 2006;163:1978–1985. [PubMed: 17074950]
3. Swedo, SE.; Snider, LA. The Neurobiology and treatment of obsessive-compulsive disorder. In: Nestler, EJ.; Charney, DS., editors. Neurobiology of Mental Illness. Oxford University Press; New York: 2004. p. 628-638.
4. Graybiel AM, Rauch SL. Toward a neurobiology of obsessive-compulsive disorder. Neuron 2000;28:343–347. [PubMed: 11144344]
5. Aouizerate B, et al. Pathophysiology of obsessive-compulsive disorder: a necessary link between phenomenology, neuropsychology, imagery and physiology. Prog. Neurobiol 2004;72:195–221. [PubMed: 15130710]
6. Hanna GL, et al. Genome-wide linkage analysis of families with obsessive-compulsive disorder ascertained through pediatric probands. Am. J. Med. Genet 2002;114:541–552. [PubMed: 12116192]
7. Shugart YY, et al. Genomewide linkage scan for obsessive-compulsive disorder: evidence for susceptibility loci on chromosomes 3q, 7p, 1q, 15q, and 6q. Mol. Psychiatry 2006;11:763–770. [PubMed: 16755275]
8. Nestadt G, et al. A family study of obsessive-compulsive disorder. Arch. Gen. Psychiatry 2000;57:358–363. [PubMed: 10768697]
9. Inouye E. Similar and dissimilar manifestations of obsessive-compulsive neurosis in monozygotic twins. Am J Psychiatry 1965;21:1171–1175. [PubMed: 14286051]
10. Carey, G.; Gottesman, II. Twin and family studies of anxiety, phobic and obsessive disorders. In: Klein, DF.; Rabkin, J., editors. Anxiety: New Research and Changing Concepts. Raven Press; New York: 1981. p. 117-136.
11. Chakrabarty K, Bhattacharyya S, Christopher R, Khanna S. Glutamatergic dysfunction in OCD. Neuropsychopharmacology 2005;30:1735–1740. [PubMed: 15841109]
12. Kim E, et al. GKAP, a novel synaptic protein that interacts with the guanylate kinase-like domain of the PSD-95/SAP90 family of channel clustering molecules. J. Cell Biol 1997;136:669–678. [PubMed: 9024696]
13. Takeuchi M, et al. SAPAPs. A family of PSD-95/SAP90-associated proteins localized at postsynaptic density. J. Biol. Chem 1997;272:11943–11951. [PubMed: 9115257]
14. Scannevin RH, Huganir RL. Postsynaptic organization and regulation of excitatory synapses. Nat. Rev. Neurosci 2000;1:133–141. [PubMed: 11252776]
15. Kim E, Sheng M. PDZ domain proteins of synapses. Nat Rev Neurosci 2004;5:771–781. [PubMed: 15378037]

16. Funke L, Dakoji S, Bredt DS. Membrane-associated guanylate kinases regulate adhesion and plasticity at cell junctions. Annu. Rev. Biochem 2005;74:219–245. [PubMed: 15952887]
17. Welch JW, Wang D, Feng G. Differential mRNA expression and protein localization of the SAP90/PSD-95-associated proteins (SAPAPs) in the nervous system of the mouse. J. Comp. Neurol 2004;472:24–39. [PubMed: 15024750]
18. Kindler S, Rehbein M, Classen B, Richter D, Bockers TM. Distinct spatiotemporal expression of SAPAP transcripts in the developing rat brain: a novel dendritically localized mRNA. Brain Res. Mol. Brain Res 2004;126:14–21. [PubMed: 15207911]
19. Malinow R, Malenka RC. AMPA receptor trafficking and synaptic plasticity. Annu. Rev. Neurosci 2002;25:103–126. [PubMed: 12052905]
20. Prybylowski K, Wenthold RJ. N-Methyl-D-aspartate receptors: subunit assembly and trafficking to the synapse. J. Biol. Chem 2004;279:9673–9676. [PubMed: 14742424]
21. Nicoll RA, Tomita S, Bredt DS. Auxiliary subunits assist AMPA-type glutamate receptors. Science 2006;311:1253–1256. [PubMed: 16513974]
22. Sheng M, Cummings J, Roldan LA, Jan YN, Jan LY. Changing subunit composition of heteromeric NMDA receptors during development of rat cortex. Nature 1994;368:144–147. [PubMed: 8139656]
23. Shi J, Aamodt SM, Constantine-Paton M. Temporal correlations between functional and molecular changes in NMDA receptors and GABA neurotransmission in the superior colliculus. J. Neurosci 1997;17:6264–6276. [PubMed: 9236237]
24. Stocca G, Vicini S. Increased contribution of NR2A subunit to synaptic NMDA receptors in developing rat cortical neurons. J. Physiol 1998;507:13–24. [PubMed: 9490809]
25. Tovar KR, Westbrook GL. The incorporation of NMDA receptors with a distinct subunit composition at nascent hippocampal synapses in vitro. J. Neurosci 1999;19:4180–4188. [PubMed: 10234045]
26. Chapman DE, Keefe KA, Wilcox KS. Evidence for functionally distinct synaptic NMDA receptors in ventromedial versus dorsolateral striatum. J. Neurophysiol 2003;89:69–80. [PubMed: 12522160]
27. Li L, Murphy TH, Hayden MR, Raymond LA. Enhanced striatal NR2B-containing - methyl-D-aspartate receptor-mediated synaptic currents in a mouse model of Huntington disease. J. Neurophysiol 2004;92:2738–46. [PubMed: 15240759]
28. Sans N, et al. A developmental change in NMDA receptor-associated proteins at hippocampal synapses. J. Neurosci 2000;20:1260–1271. [PubMed: 10648730]
29. Barria A, Malinow R. Subunit-specific NMDA receptor trafficking to synapses. Neuron 2002;35:345–53. [PubMed: 12160751]
30. Prybylowski K, et al. The synaptic localization of NR2B-containing NMDA receptors is controlled by interactions with PDZ proteins and AP-2. Neuron 47:845–857. [PubMed: 16157279]
31. van Zundert B, Yoshii A, Constantine-Paton M. Receptor compartmentalization and trafficking at glutamate synapses: a developmental proposal. Trends Neurosci 2004;27:428–37. [PubMed: 15219743]
32. Valtschanoff JG, Weinberg RJ. Laminar organization of the NMDA receptor complex within the postsynaptic density. J. Neurosci 2001;21:1211–1217. [PubMed: 11160391]
33. Day M, et al. Selective elimination of glutamatergic synapses on striatopallidal neurons in Parkinson disease models. Nat Neurosci 2006;9:251–259. [PubMed: 16415865]
34. Kreitzer AC, Malenka RC. Endocannabinoid-mediated rescue of striatal LTD and motor deficits in Parkinson's disease models. Nature 2007;445:643–647. [PubMed: 17287809]
35. Surmeier DJ, Ding J, Day M, Wang Z, Shen W. D1 and D2 dopamine-receptor modulation of striatal glutamatergic signaling in striatal medium spiny neurons. Trends Neurosci 2007;30:228–235. [PubMed: 17408758]
36. Arnold PD, et al. Association of a glutamate (NMDA) subunit receptor gene (GRIN2B) with obsessive-compulsive disorder: a preliminary study. Psychopharmacology (Berl) 2004;174:530–538. [PubMed: 15083261]
37. Arnold PD, Sicard T, Burroughs E, Richter MA, Kennedy JL. Glutamate transporter gene SLC1A1 associated with obsessive-compulsive disorder. Arch. Gen. Psychiatry 2006;63:769–776. [PubMed: 16818866]

38. Dickel DE, et al. Association testing of the positional and functional candidate gene SLC1A1/EAAC1 in early-onset obsessive-compulsive disorder. Arch. Gen. Psychiatry 2006;63:778–785. [PubMed: 16818867]
39. Feng G, et al. Dual requirement for gephyrin in glycine receptor clustering and molybdoenzyme activity. Science 1998;282:1321–1324. [PubMed: 9812897]
40. Greer JM, Capecchi MR. Hoxb8 is required for normal grooming behavior in mice. Neuron 2002;33:23–34. [PubMed: 11779477]
41. Pogorelov VM, Rodriguiz RM, Insco ML, Caron MG, Wetsel WC. Novelty seeking and stereotypic activation of behavior in mice with disruption of the DAT1 gene. Neuropsychopharmacology 2005;30:1818–1831. [PubMed: 15856082]
42. Weisstaub NV, et al. Cortical 5-HT2A receptor signaling modulates anxiety-like behaviors in mice. Science 2006;313:536–40. [PubMed: 16873667]
43. Bakeman, R.; Gottman, JM. Observing Interaction: An Introduction to Sequential Analyses. Cambridge University Press; New York: 1997. p. 56-90.
44. Treit D, Fundytus M. Thigmotaxis as a test for anxiolytic activity in rats. Pharmacol. Biochem. Behav 1988;31:959–962. [PubMed: 3252289]
45. Crawley JN, Goodwin FK. Preliminary report of a simple animal behavior model for the anxiolytic effects of benzodiazepines. Pharmacol. Biochem. Behav 1980;12:167–170. [PubMed: 6106204]
46. Feng G, et al. Imaging neuronal subsets in transgenic mice expressing multiple spectral variants of GFP. Neuron 2000;28:41–51. [PubMed: 11086982]
47. Gan WB, Grutzendler J, Wong WT, Wong RO, Lichtman JW. Multicolor “DiOlistic” labeling of the nervous system using lipophilic dye combinations. Neuron 2000;27:219–225. [PubMed: 10985343]
48. Lois C, Hong EJ, Pease S, Brown EJ, Baltimore D. Germline transmission and tissue-specific expression of transgenes delivered by lentiviral vectors. Science 2002;295:868–872. [PubMed: 11786607]
49. Parker MJ, Zhao S, Bredt DS, Sanes JR, Feng G. PSD93 regulates synaptic stability at neuronal cholinergic synapses. J. Neurosci 2004;24:378–88. [PubMed: 14724236]
50. Lau LF, Huganir RL. Differential tyrosine phosphorylation of N-methyl-D-aspartate receptor subunits. J. Biol. Chem 1995;270:20036–41. [PubMed: 7544350]

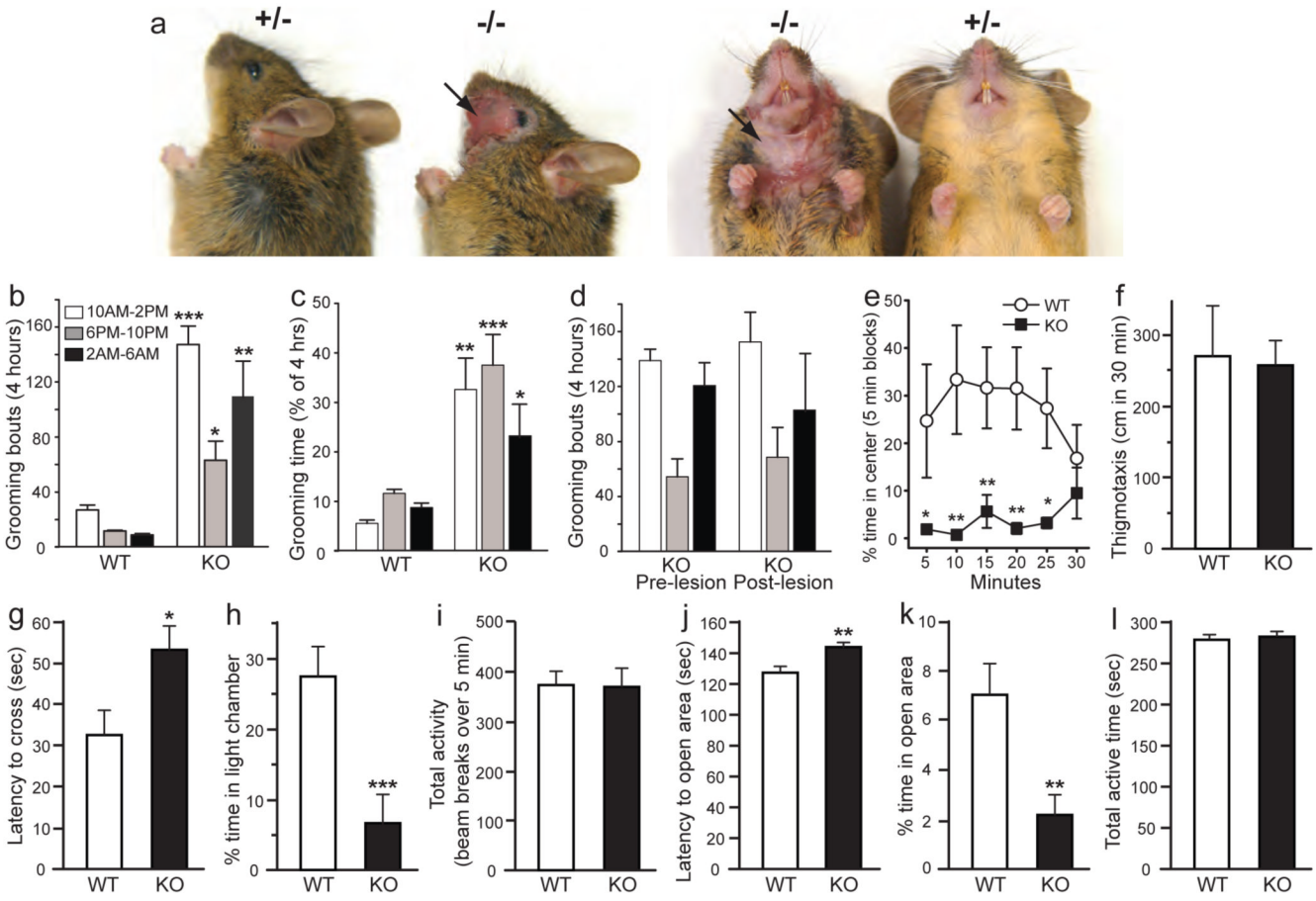

Figure 1. Facial lesions, excessive grooming and anxiety-like behaviors in SAPAP3 mutant mice

a, SAPAP3$^{-/-}$ mice have facial and neck skin lesions (arrows). **b, c,** SAPAP3$^{-/-}$ mice (KO) showed more grooming bouts (**b**) and spent more time in self-grooming (**c**) than wildtype mice (WT) at all times examined. **d,** Pre-lesion and post-lesion groups of SAPAP3$^{-/-}$ mice showed similar degrees of increased grooming. **e,f,** In the open field test, SAPAP3$^{-/-}$ mice spent less time in the center (**e**), whereas locomotion along the perimeter was comparable to wildtype controls (**f**). **g-i,** In the dark-light emergence test, SAPAP3$^{-/-}$ mice took longer to cross from the dark to the brightly lit chamber (**g**) and spent less time in the brightly lit chamber (**h**), while total activity in both chambers was similar (**i**). **j-l,** In the elevated zero maze, SAPAP3$^{-/-}$ mice took longer to cross into the open areas (**j**) and spent less time in these areas than wildtype controls (**k**), while total activity in both open and closed areas was similar (**l**). *$p < 0.05$, **$p < 0.01$, ***$p < 0.001$, repeated measures ANOVA for b-e and two-tailed t-test for f-l; all data are presented as means ± SEM from 8-9 mice per genotype, Cohen's kappa for intra-observer agreement exceeded 0.92.

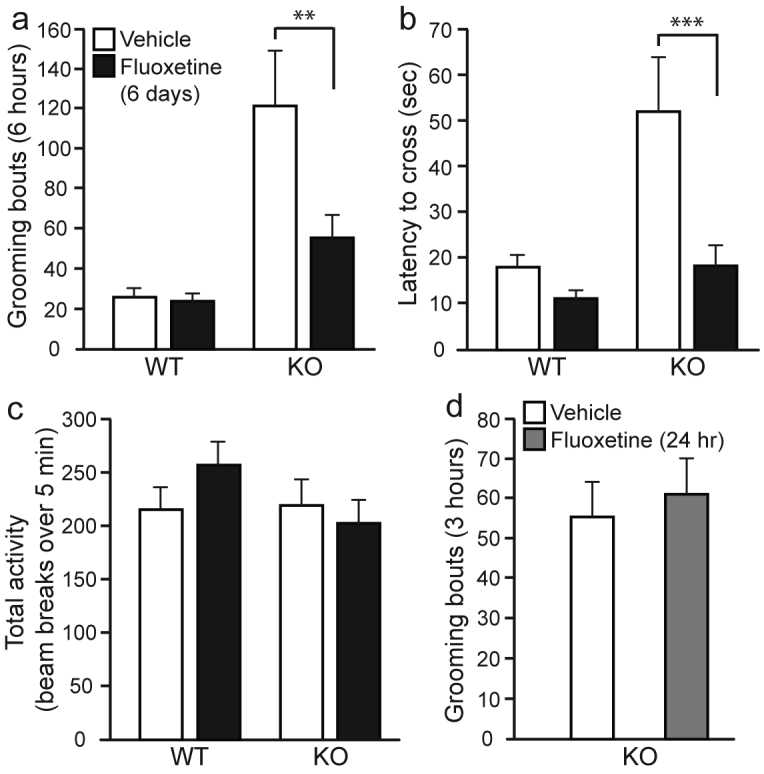

Figure 2. Fluoxetine treatment alleviates excessive grooming and anxiety-like behavior

a, Daily fluoxetine treatment (5 mg/kg, i.p.) over 6 days reduced grooming behavior in SAPAP3$^{-/-}$ mice. **b, c,** Given over 6 days, fluoxetine alleviated anxiety-like behavior of SAPAP3$^{-/-}$ mice in the dark-light emergence test. **d,** A single injection of fluoxetine (5 mg/kg, i.p.) had no effect on the grooming behavior of SAPAP3$^{-/-}$ mice. $^{**}p < 0.01$, $^{***}p < 0.001$, repeated measures ANOVA; all data are presented as means ± SEM from 9-11 mice per group, Cohen's kappa for intra-observer agreement exceeded 0.92.

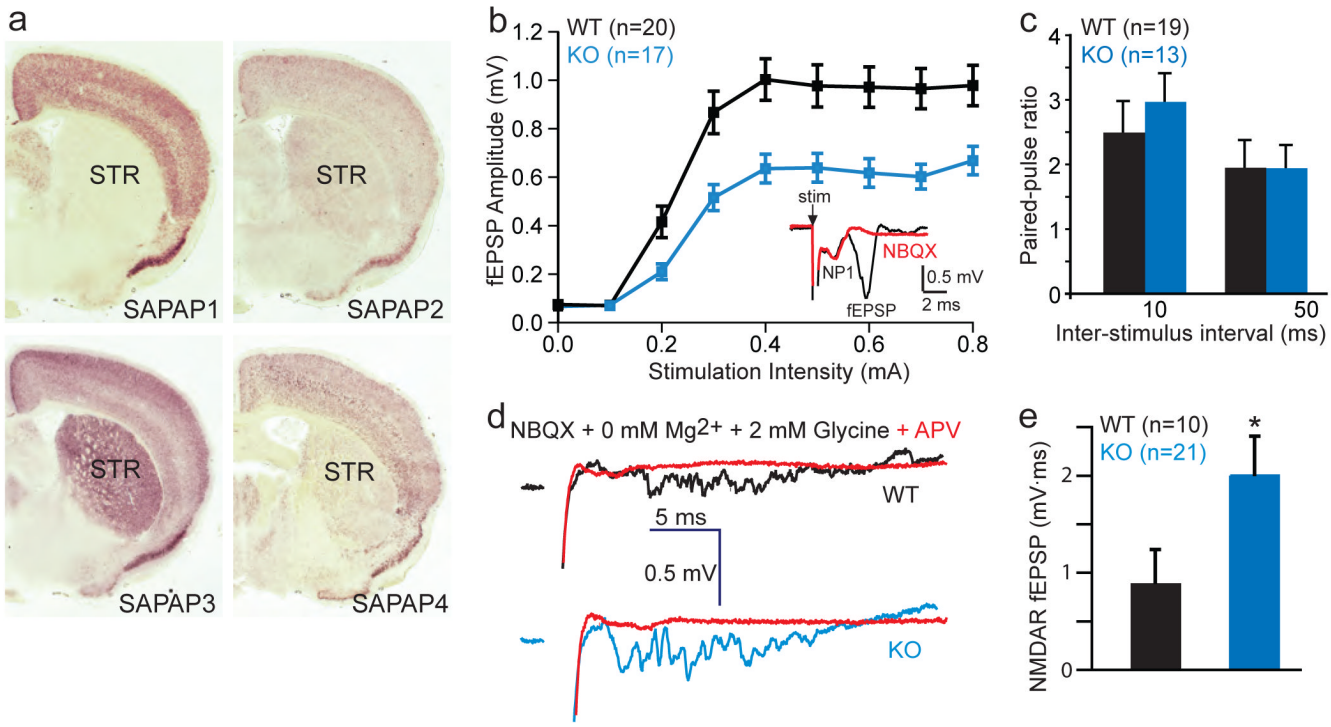

Figure 3. Altered cortico-striatal synaptic transmission in SAPAP3 mutant mice

a, Only SAPAP3 mRNA is highly expressed in the striatum (STR). **b,** Cortico-striatal field potential recordings of acute brain slices show decreased fEPSPs in SAPAP3$^{-/-}$ mice. $p < 0.001$, repeated measures ANOVA. Inset shows a typical field recording (black trace) and sensitivity to NBQX (red trace). NP1, negative peak 1. **c,** Paired-pulse ratios (slope fEPSP#2/slope fEPSP#1) are similar between wildtype and SAPAP3$^{-/-}$ mice. **d,** Example traces of NMDAR-dependent fEPSPs recorded in the presence of 50 μM NBQX, 0 mM Mg^{2+} and 2 mM glycine. Sensitivity to APV indicated by red trace. **e,** NMDAR fEPSP area is increased in SAPAP3$^{-/-}$ mice. *$p < 0.05$, two-tailed t-test; number of recordings in parentheses.

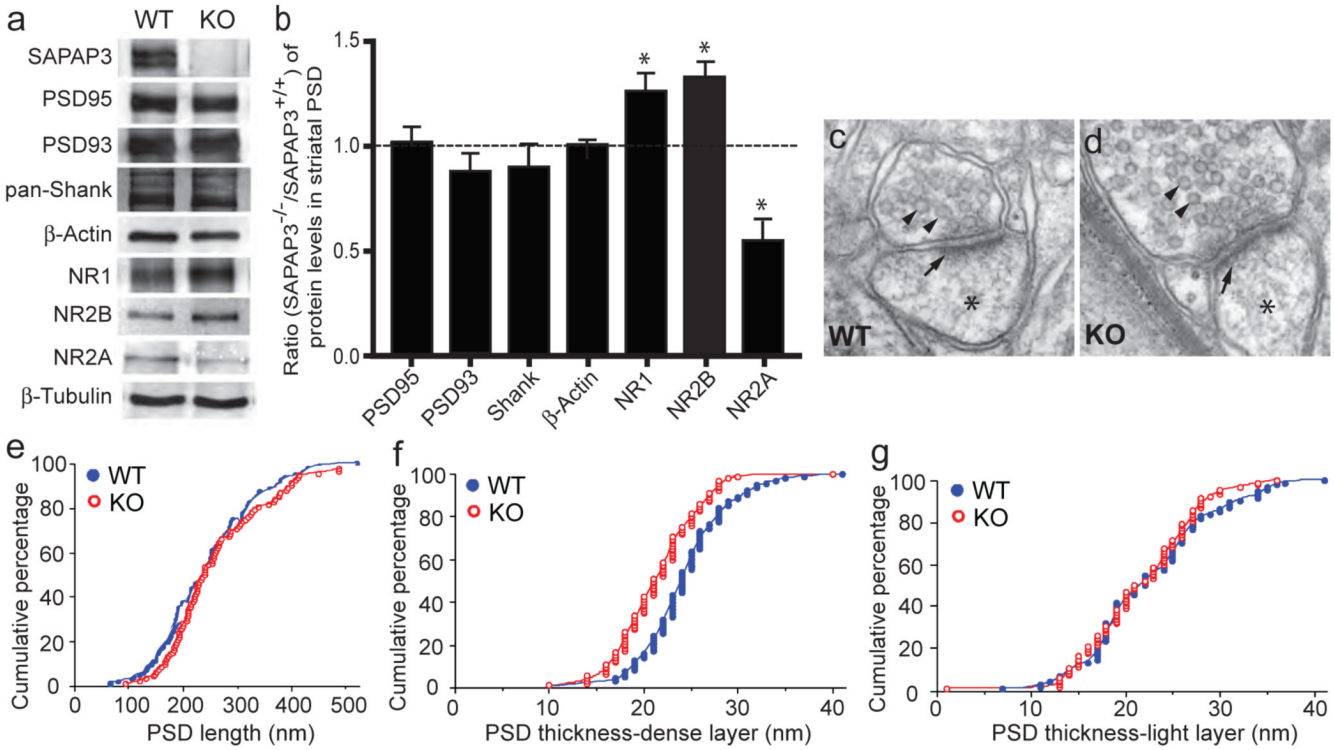

Figure 4. Structural and biochemical analyses of cortico-striatal synapses in SAPAP3 mutant mice

a, b, The levels of PSD95, PSD93 and Shank in striatal PSD fractions are not affected in SAPAP3$^{-/-}$ mice. The levels of NR1 and NR2B subunits are increased, whereas that of NR2A is decreased. β-actin and β-tubulin were used as loading controls. *$p < 0.05$, two-tailed t test. **c, d,** Electron micrographs show the presence of synaptic vesicles (arrowheads), postsynaptic densities (arrows) and dendritic spines (stars). **e,** The length of the PSD is not significantly different in wildtype and SAPAP3$^{-/-}$ mice. **f, g,** The thickness of the dense layer (**f**) of the PSD in SAPAP3$^{-/-}$ mice, but not the light layer (**g**), is reduced. $p < 0.001$, two-tailed t test; n=94 for wildtype and n=92 for SAPAP3$^{-/-}$ mice.

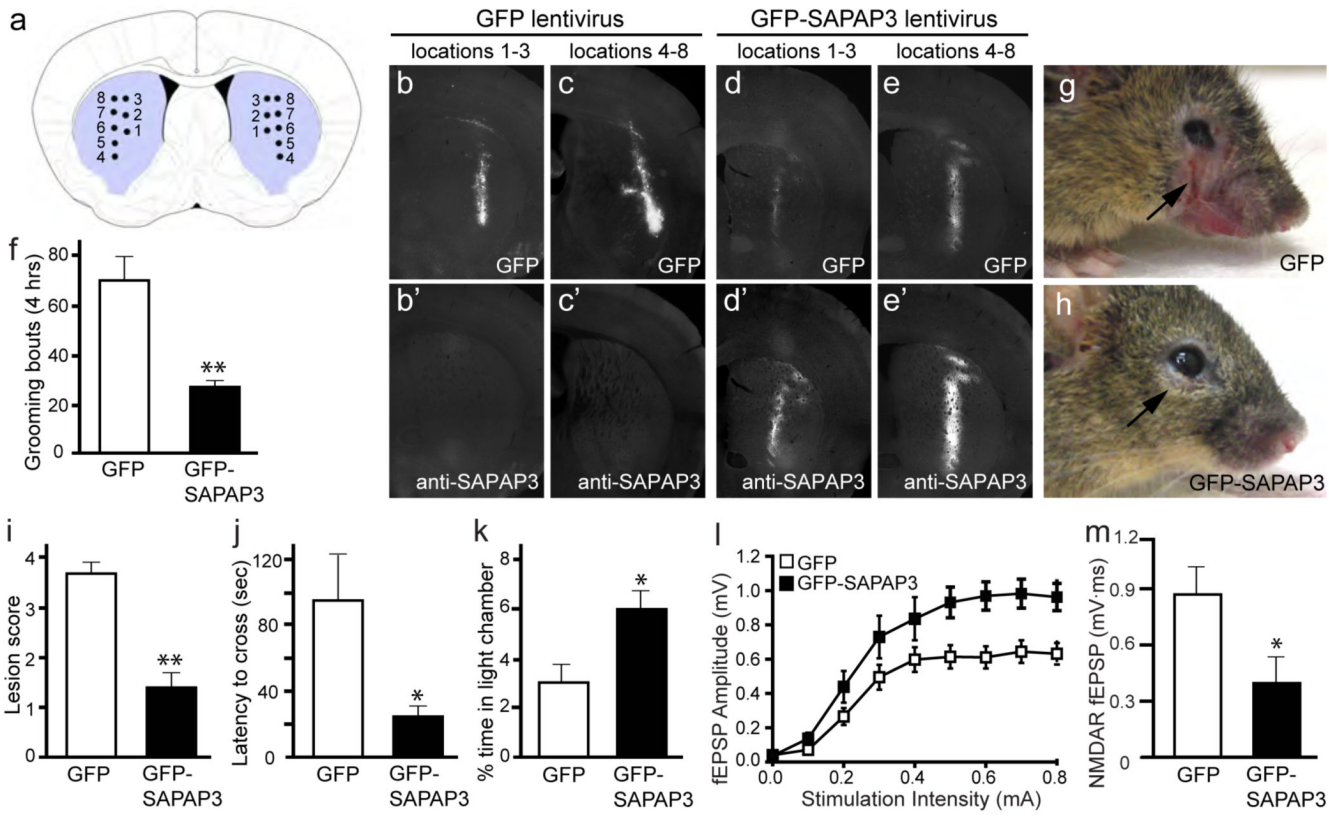

Figure 5. Lentiviral-mediated rescue of behavioral and synaptic defects in SAPAP3 mutant mice

a, Diagram showing the approximate locations of microinjections in the striatum of SAPAP3$^{-/-}$ mice. Injection site 1, locations 1-3 are more anterior than injection site 2, locations 4-8. **b-c',** Brain sections from a SAPAP3$^{-/-}$ mouse injected with GFP lentivirus show GFP fluorescence (**b, c**) and an absence of SAPAP3 staining (**b', c'**). **d-e',** Brain sections from a SAPAP3$^{-/-}$ mouse injected with GFP-SAPAP3 lentivirus show both GFP fluorescence (**d, e**) and SAPAP3 immunostaining (**d', e'**). **f,** Compared to SAPAP3$^{-/-}$ mice injected with GFP lentivirus, SAPAP3$^{-/-}$ mice injected with GFP-SAPAP3 lentivirus showed significantly reduced over-grooming behavior. $^{**}p < 0.01$, two-tailed t-test; n=8 mice/group for f, i-k. **g-h,** SAPAP3$^{-/-}$ mice injected with GFP-SAPAP3 lentivirus (**h**) had reduced severity of facial lesions when compared to SAPAP3$^{-/-}$ mice injected with GFP lentivirus (**g**). **i,** Semi-quantitative lesion scores. $^{**}p < 0.01$, Mann-Whitney U test. **j-k,** Reduced anxiety-like behaviors in SAPAP3$^{-/-}$ mice injected with GFP-SAPAP3 lentivirus in the dark-light emergence test, including decreased latency to cross from the dark to light chamber (**j**) and increased time in the light chamber (**k**). $^{*}p < 0.05$, two-tailed t-test. **l, m,** Field recordings from infected striatal area of P21-P25 SAPAP3$^{-/-}$ mice injected with GFP-SAPAP3 lentivirus showed an increase in cortico-striatal fEPSP amplitude (**l**) and a reduction of NMDAR-dependent fEPSP area (**m**). $p < 0.001$, repeated measures ANOVA for **l**; $^{*}p < 0.05$, two-tailed t-test for **m**; n is 12 and 10 for **l**, and 10 and 9 for **m** for GFP injected and GFP-SAPAP3 injected, respectively .